Electrical Control of Spin Relaxation in a Quantum Dot

S. Amasha,[1,*] K. MacLean,[1] Iuliana P. Radu,[1] D. M. Zumbühl,[2] M. A. Kastner,[1] M. P. Hanson,[3] and A. C. Gossard[3]

[1]*Department of Physics, Massachusetts Institute of Technology, Cambridge, Massachusetts 02139, USA*
[2]*Department of Physics, University of Basel, Klingelbergstrasse 82, CH-4056 Basel, Switzerland*
[3]*Materials Department, University of California, Santa Barbara, California 93106-5050, USA*

(Received 13 July 2007; published 30 January 2008)

We demonstrate electrical control of the spin relaxation time T_1 between Zeeman-split spin states of a single electron in a lateral quantum dot. We find that relaxation is mediated by the spin-orbit interaction, and by manipulating the orbital states of the dot using gate voltages we vary the relaxation rate $W \equiv T_1^{-1}$ by over an order of magnitude. The dependence of W on orbital confinement agrees with theoretical predictions, and from these data we extract the spin-orbit length. We also measure the dependence of W on the magnetic field and demonstrate that spin-orbit mediated coupling to phonons is the dominant relaxation mechanism down to 1 T, where T_1 exceeds 1 s.

DOI: 10.1103/PhysRevLett.100.046803 PACS numbers: 73.63.Kv, 03.67.Lx, 72.25.Rb, 76.30.−v

Control of the spin states of individual electrons confined in quantum dots is an important part of developing systems for applications in quantum computing and spintronics [1–3]. In a magnetic field B the spin states of the electron are split by the Zeeman energy $\Delta = |g|\mu_B B$, providing a two level quantum system that can be used as a qubit for quantum computing [1] or as the basis of spin memory [4]. Recent experiments have demonstrated the ability to manipulate [5,6] and read out [7,8] the electron's spin. An important remaining challenge is to better understand and control the interactions between the electron's spin and its solid-state environment.

The two most important of these are the hyperfine and spin-orbit interactions. The hyperfine interaction (HFI) couples the electron's spin to an effective nuclear magnetic field B_n caused by nuclear spins [9], and this causes decoherence of the spin state [5]. Methods have been suggested for suppressing this decoherence [10]. The HFI also causes relaxation [11,12], but for $B \gg B_n \approx 3$ mT this mechanism is suppressed by the mismatch between the nuclear and electron Zeeman energies.

At fields $B \gg B_n$, the spin-orbit interaction (SOI) causes spin relaxation by mixing the orbital and spin states, thus providing a mechanism for coupling the spin to electric fluctuations in the environment of the dot [13–19], primarily piezoelectric phonons [13–17]. This coupling induces spin relaxation and brings the probabilities of being in the excited and ground spin states to thermal equilibrium; at temperatures $T \ll \Delta/k_B$ an electron can relax from the excited to the ground spin state by emission of a phonon. The time scale for energy relaxation is T_1, and since relaxation necessarily destroys any coherent spin state, it sets a limit $T_2 < 2T_1$ [14]. By measuring T_1 [7,20–22] and varying the energy between the spin states, it has been shown that this mechanism accounts for relaxation between two-electron triplet and singlet states [8,23,24] in lateral GaAs dots, as well as for spin relaxation between one electron Zeeman sublevels in a layer of self-assembled Ga(In)As quantum dots [4]. At low B (but still $B \gg B_n$), where T_1 is long, other spin relaxation mechanisms may become important in lateral dots, such as SOI mediated coupling to electrical fluctuations from the Ohmic leads [17], surface gates [18], and the adjacent quantum point contact (QPC) [19] or HFI (rather than SOI) mediated coupling to phonons [25].

In this Letter we demonstrate *in situ* electrical control of the spin relaxation rate of a single electron in a lateral quantum dot by using gate voltages to manipulate the mixing of the spin and orbital states. This allows us to vary the spin relaxation rate $W \equiv T_1^{-1}$ by over an order of magnitude at fixed Δ. We find that W depends only on the confinement of the electron wave function in the direction along the applied in-plane magnetic field as expected for the SOI in GaAs, and that the dependence of W on the energy scale for confinement is that predicted by theory [13,14]. From these data we extract the spin-orbit length, which describes the strength of the SOI. We also measure W as a function of field down to 1 T, where we find that T_1 is longer than 1 s, and demonstrate that spin-orbit mediated phonon-induced spin decay is the dominant relaxation mechanism in single-electron lateral dots down to low magnetic fields.

The dot used in this work is fabricated from an $Al_{0.3}Ga_{0.7}As/GaAs$ heterostructure grown by molecular beam epitaxy. The two-dimensional electron gas (2DEG) formed at the material interface 110 nm below the surface has a density of 2.2×10^{11} cm^{-2} and a mobility of 6.4×10^5 cm^2/V s [26]. To form a single-electron dot, we apply negative voltages to Ti/Au gates patterned on the surface [Fig. 1(a)]. Adjacent to the dot is a QPC charge sensor [27]: when an electron tunnels onto the dot, the negative charge increases the resistance of the QPC, which we measure by sourcing a current I and measuring the change in voltage δV_{QPC}. We adjust the gate voltages to make the tunneling rate between the dot and lead 2 slower than the bandwidth of the charge sensing circuit (the tunneling rate to lead 1 is

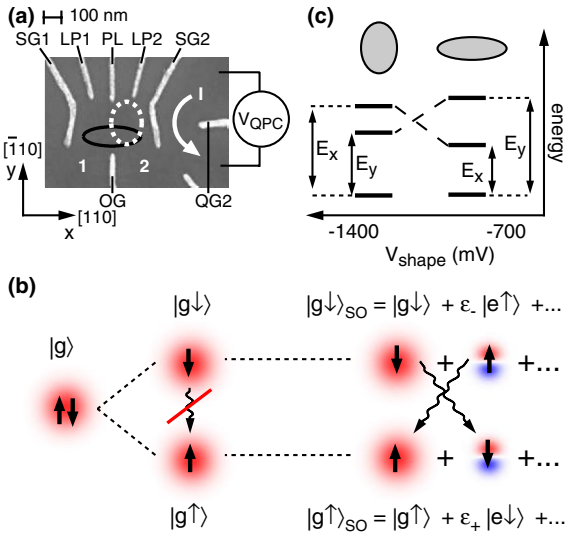

FIG. 1 (color online). (a) Electron micrograph of the gate geometry. Negative voltages are applied to the labeled gates while the unlabeled gate and the Ohmic leads (which are numbered) are kept at ground. The black solid (white dotted) ellipse illustrates the expected dot shape for less (more) negative V_{shape}. The magnetic field is parallel to the y axis and all voltage pulses are applied to gate LP2. (b) At $B = 0$ and with no SOI, the spin-$\uparrow$ and spin-$\downarrow$ states of the ground orbital state $|g\rangle$ are degenerate. Applying a magnetic field splits the spin states but phonon coupling between $|g\uparrow\rangle$ and $|g\downarrow\rangle$ is prohibited. The SOI acts as a perturbation and mixes the orbital and spin states: the perturbed spin states $|g\uparrow\rangle_{\text{SO}}$ and $|g\downarrow\rangle_{\text{SO}}$ contain excited orbital states ($|e\rangle$) of the opposite spin so the perturbed states can be coupled by phonons. The SOI involves a momentum operator and requires a change in parity for coupling of different orbital states. (c) Dot energy spectrum as gate voltages are varied to change the shape of the dot. The value of V_{shape} is the voltage on SG1 for a given set of gate voltages.

kept negligibly small). This allows us to observe electron tunneling events in real time [7,28–30]. Measurements are made in a dilution refrigerator with an electron temperature of 120 mK (unless noted otherwise), and we estimate the 2DEG is parallel to the magnetic field to within 5°.

The dominant mechanism for exchanging energy with the environment is for the electron to interact with piezoelectric phonons [13–17]. However, while phonons can couple different orbital states of the dot, they cannot couple different spin states [Fig. 1(b)]. Coupling between spin states is made possible by the SOI, which mixes the Zeeman-split ground orbital state with excited orbital states of the opposite spin [13]. This allows phonons to induce spin relaxation as illustrated in Fig. 1(b). By changing the energy of the excited orbital states, we can control the amount of SOI induced mixing and thus control the spin relaxation rate.

Using the gate voltages, we manipulate the dot shape and hence its orbital states. We model the electrostatic potential of the dot with an anisotropic harmonic oscillator potential $U(x, y) = \frac{1}{2}m^*\omega_x^2x^2 + \frac{1}{2}m^*\omega_y^2y^2$. When the voltages on all dot gates are roughly equal, one expects from the gate geometry that the dot is less confined along the x axis than along y [black solid ellipse in Fig. 1(a)]. Consequently, the lowest lying excited state is at energy $E_x = \hbar\omega_x$ above the ground state, while the next higher excited state has $E_y = \hbar\omega_y$ (assuming $E_y < 2E_x$). To change the shape of the dot, we apply a more negative voltage to gate SG1 and simultaneously apply a less negative voltage to gates LP1, PL, and LP2. The more negative voltage on SG1 pushes the dot toward SG2 and increases confinement along x, while the less negative voltage on the other gates reduces confinement along y [white dotted ellipse in Fig. 1(a)]. We use V_{shape} to indicate the set of gate voltages, although the numerical value of V_{shape} [Fig. 1(c)] is the voltage on SG1. These geometric considerations lead us to expect E_x to increase and E_y to decrease as V_{shape} is made more negative [Fig. 1(c)].

At each V_{shape} we measure the energy of the excited orbital states using a three step pulse sequence [Fig. 2(a)] with $B = 0$. After ionizing the dot, we apply a pulse V_p to bring the ground orbital state an energy $E_p = e\alpha_{\text{LP2}}V_p$ below the Fermi energy of the lead, where $e\alpha_{\text{LP2}}$ is a conversion factor we calibrate for each V_{shape} [31,32]. We find that $e\alpha_{\text{LP2}}$ increases as V_{shape} is made more negative as we expect from the geometric considerations discussed in Fig. 1. We apply the pulse for time t_p that is short (15 μs $< t_p <$ 400 μs) compared to the average tunneling time into the ground state ($\approx$10 ms near the Fermi energy), so the probability for tunneling into the ground orbital state is small. However, for sufficiently large E_p one or more excited orbital states will be below the Fermi energy. These states are more strongly coupled to the lead than the ground state [29,30], and an electron can tunnel onto the dot with rate Γ_{on}. Once on, the electron quickly decays to the ground state [20,33].

Finally, in the readout state we position the ground state just below the Fermi energy. If the dot is still ionized, then an electron tunnels onto the dot [top right in Fig. 2(a)] and we observe this with our real-time charge detection system [top panel of Fig. 2(b)]. We count the number of times N_{ion} this occurs and find N_{ion} decreases exponentially with t_p [Fig. 2(c)]. The rate of decay gives Γ_{on} and Fig. 2(d) shows Γ_{on} as a function of E_p. The two large increases correspond to the energies at which the excited orbital states cross the Fermi energy. As the excited states are pulled below the Fermi energy with increasing E_p, Γ_{on} decreases because the energy of the excited state is decreased relative to the height of the tunnel barrier [30]. Figure 2(e) shows the energies at several values of V_{shape}, and shows one state increasing and one state decreasing in energy. This behavior is what we expect from the geometric considerations: as the confinement along x increases and along y decreases with more negative V_{shape}, the energy E_x of the x-excited

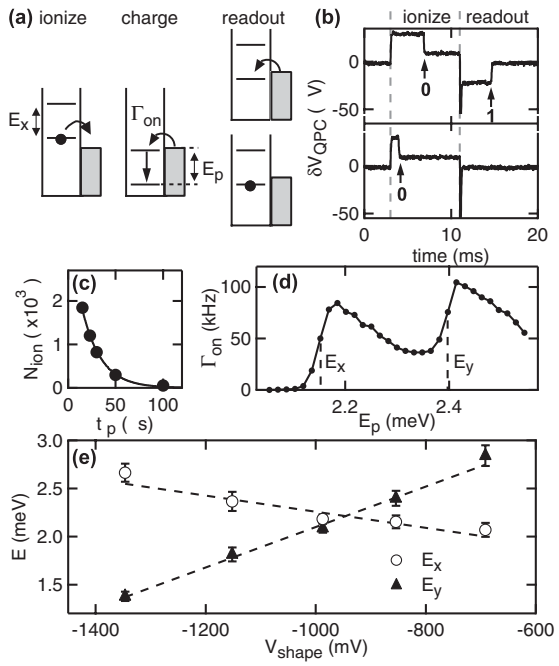

FIG. 2. (a) Three step pulse sequence for measuring the energy of the excited orbital states. (b) Examples of real-time data. The direct capacitive coupling to the pulsed gate causes the QPC to respond to the pulse sequence; electron tunneling events are evident on top of this response. The 0's denote when an electron tunnels off the dot, while 1's denote when an electron tunnels on. The charging pulse ($t_p = 50$ μs for this example) appears as a sharp spike between the ionization and readout periods. (c) The number of events N_{ion} for which the dot is empty after the charging pulse [top panel in Fig. 2(b)] as a function of t_p. The solid line is a fit to an exponential to determine the rate Γ_{on} at which electrons tunnel onto the dot. (d) Γ_{on} vs E_p for $V_{shape} = -850$ mV. The two sharp rises mark the energies when an excited state crosses the Fermi energy. (e) Energies of the excited orbital states of the dot as a function of V_{shape}. The dashed lines are linear fits to the data.

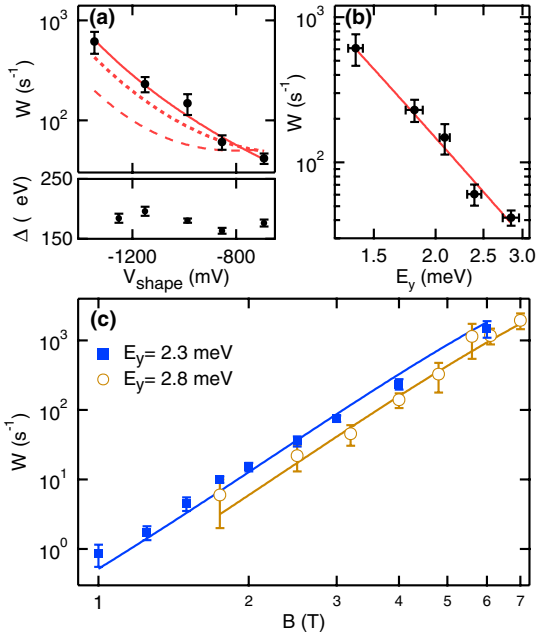

FIG. 3 (color online). (a) Top panel: W vs V_{shape} at $B = 3$ T. The solid, dotted, and dashed curves show fits with $A_x/A_y = 0.01$, 0.25, and 1, respectively. Bottom panel: Δ vs V_{shape} at $B = 7.5$ T where the Zeeman splitting is large and can easily be determined by measuring the positions of the increases in Γ_{on} as the ground and excited spin states are pulsed below the Fermi energy of the lead [35]. (b) The same relaxation rate data as in Fig. 3(a), plotted as a function of E_y. The solid line is a fit to find the spin-orbit length as discussed in the text. (c) Spin relaxation rate as a function of magnetic field for two different sets of gate voltages. Solid lines are fits discussed in the text.

state increases, while the energy E_y of the y-excited state decreases, allowing us to identify the x and y states as indicated in Fig. 2(e). This orientation of the dot orbital states is also consistent with measurements of W discussed next.

For each V_{shape}, we measure $W \equiv T_1^{-1}$ at $B = 3$ T. To do this, we first ionize the dot and then pulse both Zeeman-split levels below the Fermi level for a time t_w. During this time electrons can tunnel onto the dot and then relax from the excited to the ground spin state. By measuring the decay of the probability of being in the excited spin state as a function of t_w, we obtain W [22]. The results are shown in Fig. 3(a) demonstrating that we can electrically control W by over an order of magnitude. We have verified that the Zeeman splitting does not vary with V_{shape} [Fig. 3(a)], confirming the observed variation is not caused by changes in Δ.

The energy of the excited orbital states affect W because the higher the energy of the excited states, the weaker the SOI coupling to the ground state, and the slower the relaxation rate. If we model W assuming the potential $U(x, y)$ given above, an in-plane B, a SOI that is linear in the electron's momentum, and a phonon wavelength much greater than the dot size, then $W = A_x E_x^{-4} + A_y E_y^{-4}$. Here A_x and A_y describe the contribution of each orbital to spin relaxation and $W \propto E^{-4}$ because of van Vleck cancellation [13]. We fit the data in Fig. 3(a) to this equation by approximating $E_x(V_{shape})$ and $E_y(V_{shape})$ by the dashed lines shown in Fig. 2(e). The results are shown in Fig. 3(a), and we find that $A_x/A_y < 0.14$, implying that only the y-excited orbital state is contributing to spin relaxation.

We can understand why the y-excited state dominates spin relaxation from the spin-orbit Hamiltonian. In the coordinate system from Fig. 1(a) it takes the form $H_{SO} = (\beta - \alpha)p_y\sigma_x + (\beta + \alpha)p_x\sigma_y$ where α and β are the Rashba and Dresselhaus spin-orbit parameters, respectively [14]. B is applied along the y axis so only the first term in H_{SO}, which is proportional to σ_x, can couple

different spin states as in Fig. 1(b). Since this term is proportional to p_y, a change in parity along the y axis is also required. The x-excited state does not satisfy this requirement, so the $p_y\sigma_x$ term couples the Zeeman-split ground orbital state to y-excited states of opposite spin. A consequence is that for $V_{\text{shape}} > -1000$ mV, it is the higher energy excited state that determines W, an unusual situation.

For a comparison to theory, Fig. 3(b) shows W as a function of E_y; here the directly measured values of E_y are used. In the limit where the phonon wavelength is much larger than the size of the dot, $W \approx AB^5E_y^{-4}\lambda_{\text{SO}}^{-2}$ where $A = 33\ \text{s}^{-1}\,\text{meV}^4\,\mu\text{m}^2/T^5$ depends on $|g|$ and phonon parameters in GaAs, and $\lambda_{\text{SO}} = \hbar/m^*|\beta - \alpha|$. We fit the data in Fig. 3(b) to a theoretical prediction by Golovach *et al.* [14] that includes the effects of the phonon wavelength being comparable to the size of the dot and obtain $\lambda_{\text{SO}} = 1.7 \pm 0.2\ \mu$m, consistent with previous measurements in dots [34]. We note that taking E_x instead of E_y, i.e., a different dot orientation, to explain the spin relaxation would be inconsistent with the data (W would increase with increasing E_x), independently confirming the dot orientation.

Spin relaxation also depends sensitively on the magnetic field [4] as shown in Fig. 3(c) for two different sets of gate voltages. At 1 T, W is less than 1 s^{-1}, corresponding to a very long $T_1 > 1$ s. These data demonstrate electrical control of W over a range of fields. Using the previously determined λ_{SO}, we can independently estimate E_y for the two sets of gate voltages by fitting the data to the theory of Golovach *et al.* [14]. The solid lines in Fig. 3(c) show the fit results, and we obtain values of E_y consistent with the values that we expect, which are 2.2 ± 0.2 meV (solid squares) and 2.9 ± 0.3 meV (open circles). Moreover, the agreement between our data and theory down to a field of 1 T demonstrates that spin-orbit mediated coupling to piezoelectric phonons is the dominant mechanism down to low fields, corresponding to very long times.

In summary, we have demonstrated electrical control of the spin relaxation rate of a single electron in a lateral quantum dot by manipulating the orbital states *in situ* using gate voltages. The measured dependence of W on orbital confinement and magnetic field is in excellent agreement with theory [13,14], demonstrating that spin-orbit mediated coupling to phonons is the dominant spin relaxation mechanism.

We are grateful to V. N. Golovach, D. Loss, and L. Levitov for discussions, to V. N. Golovach for providing his code to perform calculations, and to I. J. Gelfand and T. Mentzel for experimental help. This work was supported by the U.S. Army Research Office under Grant No. W911NF-05-1-0062, by the National Science Foundation under Grant No. DMR-0353209, and in part by the NSEC Program of the National Science Foundation under Grant No. PHY-0117795.

*samasha@mit.edu

[1] D. Loss and D. P. DiVincenzo, Phys. Rev. A **57**, 120 (1998).
[2] D. D. Awschalom and M. E. Flatté, Nature Phys. **3**, 153 (2007).
[3] R. Hanson *et al.*, Rev. Mod. Phys. **79**, 1217 (2007).
[4] M. Kroutvar *et al.*, Nature (London) **432**, 81 (2004).
[5] J. R. Petta *et al.*, Science **309**, 2180 (2005).
[6] F. H. L. Koppens *et al.*, Nature (London) **442**, 766 (2006).
[7] J. M. Elzerman *et al.*, Nature (London) **430**, 431 (2004).
[8] R. Hanson *et al.*, Phys. Rev. Lett. **94**, 196802 (2005).
[9] A. V. Khaetskii, D. Loss, and L. Glazman, Phys. Rev. Lett. **88**, 186802 (2002); K. Ono and S. Tarucha, Phys. Rev. Lett. **92**, 256803 (2004); F. H. L. Koppens *et al.*, Science **309**, 1346 (2005).
[10] D. Klauser, W. A. Coish, and D. Loss, Phys. Rev. B **73**, 205302 (2006); G. Giedke *et al.*, Phys. Rev. A **74**, 032316 (2006); D. Stepanenko *et al.*, Phys. Rev. Lett. **96**, 136401 (2006).
[11] I. A. Merkulov, Al. L. Efros, and M. Rosen, Phys. Rev. B **65**, 205309 (2002).
[12] A. C. Johnson *et al.*, Nature (London) **435**, 925 (2005).
[13] A. V. Khaetskii and Y. V. Nazarov, Phys. Rev. B **64**, 125316 (2001).
[14] V. N. Golovach, A. Khaetskii, and D. Loss, Phys. Rev. Lett. **93**, 016601 (2004).
[15] V. I. Fal'ko, B. L. Altshuler, and O. Tsyplyatyev, Phys. Rev. Lett. **95**, 076603 (2005).
[16] P. Stano and J. Fabian, Phys. Rev. Lett. **96**, 186602 (2006).
[17] P. San-Jose *et al.*, Phys. Rev. Lett. **97**, 076803 (2006).
[18] F. Marquardt and V. A. Abalmassov, Phys. Rev. B **71**, 165325 (2005).
[19] M. Borhani, V. N. Golovach, and D. Loss, Phys. Rev. B **73**, 155311 (2006).
[20] T. Fujisawa *et al.*, Nature (London) **419**, 278 (2002).
[21] R. Hanson *et al.*, Phys. Rev. Lett. **91**, 196802 (2003).
[22] S. Amasha *et al.*, arXiv:cond-mat/0607110.
[23] S. Sasaki *et al.*, Phys. Rev. Lett. **95**, 056803 (2005).
[24] T. Meunier *et al.*, Phys. Rev. Lett. **98**, 126601 (2007).
[25] S. I. Erlingsson and Y. V. Nazarov, Phys. Rev. B **66**, 155327 (2002).
[26] G. Granger *et al.*, Phys. Rev. B **72**, 165309 (2005).
[27] M. Field *et al.*, Phys. Rev. Lett. **70**, 1311 (1993).
[28] W. Lu *et al.*, Nature (London) **423**, 422 (2003).
[29] S. Gustavsson *et al.*, Phys. Rev. Lett. **96**, 076605 (2006).
[30] K. MacLean *et al.*, Phys. Rev. Lett. **98**, 036802 (2007).
[31] We calibrate $e\alpha_{\text{LP2}}$ by measuring the width of the Fermi function of Ohmic lead 2 at 300 mK.
[32] S. Gustavsson *et al.*, Phys. Rev. B **74**, 195305 (2006).
[33] J. I. Climente *et al.*, Phys. Rev. B **74**, 035313 (2006).
[34] D. M. Zumbühl *et al.*, Phys. Rev. Lett. **89**, 276803 (2002).
[35] S. Amasha *et al.*, arXiv:cond-mat/0709.1730.